

Function Recovery Attacks in Gate-Hiding Garbled Circuits using SAT Solving

Chao Yin^{1,2}, Zunchen Huang², Chenglu Jin², Marten van Dijk^{1,2}, Fabio Massacci^{1,3}

¹Vrije University, Amsterdam

²Centrum Wiskunde & Informatica, Amsterdam

³University of Trento, Italy

{Chao.Yin, Zunchen.Huang, Chenglu.Jin, Marten.van.Dijk}@cwi.nl,
fabio.massacci@ieee.org

Abstract

Semi-Private Function Evaluation enables joint computation while protecting both input data and function logic. A practical instantiation is gate-hiding garbled circuits, which conceal gate functionalities while revealing the circuit topology. Existing security definitions intentionally exclude leakage through circuit topology, leaving the concrete impact of such leakage on function privacy insufficiently understood.

We analyze the empirical security of gate hiding under two adversarial models that capture realistic computational capabilities. We present a SAT-based function-recovery attack that reconstructs hidden gate operations from a circuit's public topology. To enable recovery on larger and more complex circuits, we develop an incremental SAT-solving framework combined with a set of composable, topology-preserving simplification theorems. These techniques jointly reduce the SAT instance size and progressively constrain the search space across repeated solving iterations.

We evaluate our attack on ISCAS benchmarks, representative secure computation circuits, and fault-tolerant sensor fusion circuits under a fixed 24-hour recovery budget. Compared to baseline approaches, our optimized attack achieves up to a 159-fold speedup in recovery time without increasing the number of oracle queries. Our results demonstrate that topology leakage alone can enable effective function recovery in practice.

CCS Concepts

- **Security and privacy** → **Cryptanalysis and other attacks; Logic and verification;**
- **Theory of computation** → **Automated reasoning; Cryptographic protocols;**
- **Mathematics of computing** → **Solvers.**

Keywords

Gate-hiding garbled circuits, SAT attack, Reverse engineering

Permission to make digital or hard copies of all or part of this work for personal or classroom use is granted without fee provided that copies are not made or distributed for profit or commercial advantage and that copies bear this notice and the full citation on the first page. Copyrights for components of this work owned by others than the author(s) must be honored. Abstracting with credit is permitted. To copy otherwise, or republish, to post on servers or to redistribute to lists, requires prior specific permission and/or a fee. Request permissions from permissions@acm.org.

Conference'17, Washington, DC, USA

© 2026 Copyright held by the owner/author(s). Publication rights licensed to ACM.

ACM ISBN 978-x-xxxx-xxxx-x/YY/MM

<https://doi.org/10.1145/nnnnnnnnnnnnnn>

ACM Reference Format:

Chao Yin^{1,2}, Zunchen Huang², Chenglu Jin², Marten van Dijk^{1,2}, Fabio Massacci^{1,3}, ¹Vrije University, Amsterdam, ²Centrum Wiskunde & Informatica, Amsterdam, ³University of Trento, Italy, {Chao.Yin, Zunchen.Huang, Chenglu.Jin, Marten.van.Dijk}@cwi.nl, fabio.massacci@ieee.org . 2026. Function Recovery Attacks in Gate-Hiding Garbled Circuits using SAT Solving. In . ACM, New York, NY, USA, 16 pages. <https://doi.org/10.1145/nnnnnnnnnnnnnn>

1 Introduction

Unlike standard secure multi-party computation, which assumes the function to be public and only protects the parties' inputs, *private function evaluation* (PFE) aims to protect both the input data and the function being evaluated [13]. Achieving such strong privacy in general-purpose settings remains costly in practice. Existing PFE protocols typically reduce private-function computation to secure computation of a public circuit, which requires transforming a circuit of size n into a universal circuit of size $\Theta(n \log n)$ [8, 27]. Although asymptotically optimal, this expansion introduces substantial overhead and remains a performance bottleneck.

Katz and Malka [5] avoided universal circuits using singly homomorphic public-key encryption, but their protocol remains costly in practice. More recently, *fully homomorphic encryption* (FHE) has been used to evaluate encoded representations of functions using homomorphic lookup tables and related techniques, without resorting to universal circuits [9, 10, 29]. These FHE-based approaches improve expressiveness for PFE, but still inherit the high computational cost of FHE, including large ciphertexts, expensive key-switching and rotations, and (in generic settings) the overhead of bootstrapping [18, 26]. Taken together, these results suggest that achieving full function privacy in general remains costly in practice and motivate relaxed notions such as *semi-private function evaluation* (Semi-PFE).

Semi-PFE was introduced as a practical alternative to full PFE by relaxing function privacy to allow limited structural leakage [2, 3, 11, 14]. A prominent instantiation of Semi-PFE is *Gate-Hiding* (GH) garbled circuits, which intentionally reveal the circuit topology while hiding the type of each gate [6, 16, 17, 21]. The textbook Yao garbling scheme already satisfies gate hiding, as gate types are indistinguishable to the evaluator under a standard hybrid argument. Subsequent work showed that this property extends to optimized constructions such as Free-XOR without increasing asymptotic cost, and formalized GH as the requirement that a garbling leaks only the circuit topology while concealing each gate's truth table [16]. Research has since focused on reducing constant factors

in GH, culminating in unified constructions that support all two-input Boolean functions with near-optimal per-gate costs [17].

Yet, these efficiency gains hold under a security model that treats topology leakage as acceptable. Elsewhere, revealing the circuit structure have enabled efficient attacks. In hardware gate camouflaging, where an adversary observes the complete netlist while each camouflaged gate may implement one of several possible functions, SAT-based attacks have been successful. For example, El Mas-sad et al. [1] showed that, given oracle access, a SAT solver can recover camouflaged gate identities in the ISCAS benchmarks.

Still, existing hardware attacks assume strong attacker knowledge: each camouflaged gate is typically restricted to a small set of candidate functions, and *the vast majority of gates are known*. In contrast, *GH garbled circuits hide all gates*, each of which may realize any of the sixteen two-input Boolean functions. Whether the circuit topology exposed by GH constructions enables practical function recovery is the focus of this work.

1.1 Our Contributions

We show that revealing the circuit topology alone can suffice to recover the underlying function in practical settings. Our empirical results challenge the common intuition in semi-private function evaluation that, when only the circuit topology is revealed, function recovery is feasible only via exhaustive search. This intuition is reflected, for example, in the discussion¹ by Paus et al. [14].

(i) We show that circuit topology alone imposes strong constraints on possible gate-type assignments. Using only the circuit topology, we can restrict the set of admissible gate types at each gate while preserving the overall input–output behavior of the circuit. As a result, for k such gates, an adversary needs to consider only 8^k , 6^k or 3^k possible gate-type assignments, instead of the 16^k gate-type assignments allowed by gate-hiding schemes [17].

(ii) We develop the first SAT-based function recovery attack tailored to gate-hiding garbled circuits. Our innovations extend SAT-based gate decamouflaging to the GH setting in which *all* gates semantics are hidden cryptographically and each gate may realize any of the sixteen two-input Boolean functions.

(iii) Under a fixed 24-hour time budget, we demonstrate that our attack can recover on AWS off-the-shelf hardware a functionally equivalent gate-type assignment for a diverse set of circuits with hundreds of gates and hundreds of inputs bits using limited oracle queries. While these circuit sizes are still smaller than real-world deployments, our results provide the first empirical evidence that circuit topology leakage can be algorithmically exploited to enable practical function recovery in GH schemes.

Paper organization. We begin by defining the system and threat models (§2) and formulate the function recovery problem (§3). We then present a set of topology-preserving simplification theorems that exponentially reduce the search space (§4), followed by our SAT-based formulation of the function recovery task (§5). Next, we describe the baseline attack, obtained by generalizing the NDSS 15 decamouflaging attack [1] to our setting (§6), and introduce our

¹Quoted verbatim from [14]: Clearly, if this is not large enough (i.e., if the number of PPBs n or number of possible functionalities of PPBs $|F|$ is small), evaluator Alice might guess the correct function with high probability or probe the system via exhaustive search which must be prohibited by other means.

optimized incremental variant (§7). We further extend the attack to the setting where the adversary controls only a subset of the inputs (§8). We then describe the circuit benchmarks used in our evaluation (§9). Finally, we report experimental results (§10), analyze point–function behavior (§11), present related work (§12), discuss the limitations of the work (§13), and conclude the paper (§14).

Artifact Availability Statement. Netlists of circuits, SAT encodings, Python code and experimental data is available anonymously for review and will be available on Zenodo upon acceptance.

2 System Model and Threat model

2.1 GH Semi-PFE System model

We consider a two-party Semi-PFE setting involving a function owner Alice and an evaluator Bob. Alice is the sole party with knowledge of the Boolean function f , represented as a Boolean circuit. Bob holds a private input and participates in the evaluation of f without learning the function (except the I/O pairs that he asked to compute). In the GH model, Bob knows the circuit topology of f , including the number of gates, their wiring, and the ordering of each gate’s input wires, but not the type of any gate which may implement any of the sixteen two-input Boolean functions [17].

The computation is realized using GH garbled circuits. Alice garbles the circuit in a way that preserves the original topology while hiding all gate types, and provides Bob with the resulting garbled circuit. Bob obtains the garbled input labels corresponding to his input via oblivious transfer and evaluates the garbled circuit gate by gate. At the end of the evaluation, Bob learns the output of the computation and nothing beyond what can be inferred from the output and the circuit topology.

2.2 Threat model

We consider Bob as the adversary and assume an honest-but-curious setting. Bob follows the GH Semi-PFE protocol as specified, but attempts to recover the private function f .

As a legitimate evaluator, Bob has black-box oracle access to the function through repeated protocol executions. That is, Bob may adaptively choose inputs and observe the corresponding outputs, while having no access to intermediate wire values. We do not impose protocol-level restrictions on the number of evaluations; however, we consider only attacks that use a number of oracle queries that is significantly smaller than the full input space size 2^n . Recovering any gate-type assignment that is functionally equivalent to the original circuit is considered a successful attack.

Bob’s private inputs are not revealed to Alice as input privacy is guaranteed by the underlying cryptographic protocol.

Threat Model A (Evaluator-Only Input). In Threat Model A, Bob supplies inputs x to the evaluation and observes the corresponding outputs $f(x)$. Bob obtains one or more input–output pairs $(x, f(x))$ and attempts to recover a gate-type assignment consistent with the observed oracle behavior.

Threat Model B (Partial Input Knowledge). In Threat Model B, the target function takes two inputs and is written as $f(x, y)$, where x is known to Bob and y is an unknown but fixed secret throughout the attack. Bob knows the input domain of y , but not its value. Bob

may adaptively choose inputs x and observe the corresponding outputs $f(x, y)$. From Bob's perspective, this setting is equivalent to reverse-engineering a circuit with a fixed but unknown input.

3 The Function Recovery Problem

We denote by \mathcal{L} the library of all sixteen possible two-input Boolean gate types, $\mathcal{L} = \{\text{AND}, \text{NAND}, \text{OR}, \dots\}$. State-of-the-art gate-hiding schemes can encode any gate type in \mathcal{L} . The circuit is modeled as a directed ordered acyclic graph (DAG), where the ordering captures the distinction between the two input wires of each gate.

Definition 3.1. Let $C = \{\mathcal{N} \cup I \cup O, E, \mathcal{T}\}$ be the target circuit, where $\mathcal{N} = \{g_0, g_1, \dots, g_{k-1}\}$ is the set of gate nodes, I denotes the set of external input nodes, and O denotes the set of output nodes. The edge set $E \subseteq (I \cup \mathcal{N}) \times (\mathcal{N} \cup O)$ specifies the directed wiring between nodes, and the mapping $\mathcal{T} : \mathcal{N} \rightarrow \mathcal{L}$ assigns each gate node a two-input Boolean gate type. Under the assignment \mathcal{T} , the circuit computes a Boolean function $\text{Eval}(C) : \{0, 1\}^n \rightarrow \{0, 1\}^m$, which maps each input vector \mathbf{x} to the corresponding output vector \mathbf{z} via evaluation along the edges in E .

We denote by $\tau(C) = (\mathcal{N} \cup I \cup O, E)$ the circuit topology, that is, the structure of the circuit without gate-type assignments. Conversely, equipping a topology $\tau(C)$ with a gate-type assignment \mathcal{T} yields a fully instantiated circuit C . We denote black-box access to the circuit C via function $\text{Oracle}_f(\cdot)$. On input \mathbf{x} , the oracle returns the corresponding output $\mathbf{z} = \text{Oracle}_f(\mathbf{x})$.

We now formalize function recovery under Threat Model A: the attacker has adaptive black-box oracle access to the target circuit.

Problem 1 (Function Recovery in Model A). Let the target Boolean circuit be $C = (\tau, \mathcal{T})$, where $\tau = (\mathcal{N} \cup I \cup O, E)$. The attacker is given the circuit topology τ , does not know the gate-type assignment \mathcal{T} , but may interact with the oracle $\text{Oracle}_f(\cdot)$ adaptively. The target function remain fixed throughout the attack.

Formal Goal. In each query round i , the attacker selects an input vector $\mathbf{x}^{(i)} \in \{0, 1\}^n$ and receives the corresponding output $\mathbf{z}^{(i)} = \text{Oracle}_f(\mathbf{x}^{(i)}) \in \{0, 1\}^m$, it must recover a gate-type assignment $\mathcal{T}' : \mathcal{N} \rightarrow \mathcal{L}$ such that the instantiated circuit $C' = (\tau, \mathcal{T}')$ is functionally equivalent to C , i.e.,

$$\forall \mathbf{x} \in \{0, 1\}^n : \text{Eval}(C')(\mathbf{x}) = \text{Eval}(C)(\mathbf{x}) = \text{Oracle}_f(\mathbf{x})$$

Any such \mathcal{T}' is considered a successful recovery.

Query Efficiency Criterion. The attacker aims to recover a valid assignment \mathcal{T}' using a number of oracle queries that is significantly smaller than the exhaustive bound 2^n . The primary complexity measures are the number of oracle queries $|\mathcal{Q}|$ and the computational cost required to derive \mathcal{T}' . Formally, the recovery is based on a query set $\mathcal{Q} = \{(\mathbf{x}, \text{Oracle}_f(\mathbf{x})) \mid \mathbf{x} \in \mathcal{X}\}$, where $\mathcal{X} \subseteq \{0, 1\}^n$ and $|\mathcal{Q}| \ll 2^n$.

We now consider Threat Model B, which extends the problem by assuming that the circuit input of total length $n + n'$ is split into two parts. The adversary controls the input $\mathbf{x} \in \{0, 1\}^n$ while the remaining n' -bit input \mathbf{y} is fixed but unknown to the adversary. The circuit output remains m bits.

Problem 2 (Function Recovery in Model B). Let the target Boolean circuit be given by $C = (\tau, \mathcal{T})$, where $\tau = (\mathcal{N} \cup I \cup O, E)$. The adversary is given the circuit topology τ but does not know the gate-type

assignment \mathcal{T} nor the value of the fixed input \mathbf{y} . The adversary may interact with the oracle $\text{Oracle}_{f,y}(\cdot)$ adaptively.

Formal Goal. Each query consists of an input $\mathbf{x} \in \{0, 1\}^n$, and the oracle returns $\text{Oracle}_{f,y}(\mathbf{x}) = \text{Eval}(C)(\mathbf{x}, \mathbf{y}) \in \{0, 1\}^m$, where $\mathbf{y} \in \{0, 1\}^{n'}$ is fixed throughout the attack, recover a gate-type assignment $\mathcal{T}' : \mathcal{N} \rightarrow \mathcal{L}$ together with a candidate value $\mathbf{y}' \in \{0, 1\}^{n'}$ such that the instantiated circuit $C' = (\tau, \mathcal{T}')$ is functionally equivalent to the target circuit under the fixed input, i.e.

$$\forall \mathbf{x} \in \{0, 1\}^n, \text{Eval}(C')(\mathbf{x}, \mathbf{y}') = \text{Eval}(C)(\mathbf{x}, \mathbf{y}) = \text{Oracle}_{f,y}(\mathbf{x}).$$

Multiple pairs $(\mathcal{T}, \mathbf{y})$ may instantiate the same functionality over the attacker-controllable input domain. Any such pair $(\mathcal{T}', \mathbf{y}')$ that is functionally equivalent to the oracle on all inputs $\mathbf{x} \in \{0, 1\}^n$ is considered a valid recovery.

Treatment of NOT Gates. W.l.o.g. we assume that NOT gates do not appear in the circuit. Since \mathcal{L} contains all sixteen two-input Boolean functions, any NOT gate can be absorbed into an adjacent two-input gate by complementing the corresponding wire value (including at primary inputs or outputs), without introducing new gates or changing the topology. Accordingly, we focus on hiding and recovering the types of two-input gates.

4 Gate Search Space Simplification

Recovering an unknown Boolean circuit from oracle access can be viewed as a search problem over gate-type assignments that are consistent with the observed input-output (I/O) behavior and the given topology. For a circuit with k gates drawn from the full two-input Boolean gate library \mathcal{L} of 16 primitive functions, the naive search space contains $|\mathcal{L}|^k = 16^k$ possible assignments that renders exhaustive exploration infeasible, even for circuits of moderate size.

By analyzing local structural patterns of the revealed topology, and applying topology-preserving logical equivalences, we identify classes of gates whose admissible types can be restricted to much smaller subsets of \mathcal{L} (e.g. of size 3 or 6) without affecting the circuit's overall I/O behavior. These restrictions yield an exponential reduction in the adversary's search space. These topology-preserving simplification results form the algorithmic foundation of our optimized SAT-based function recovery attack (§7).

4.1 Forward Propagation Reduction

The forward-propagation simplification exploits the fact that a Boolean negation at a gate's output can be pushed to its downstream consumers without changing the circuit's behavior or topology. An inverted output can be absorbed by reinterpreting the gate as its complemented variant (e.g., AND as NAND) and propagating the inversion forward. Iteratively applying this process pushes all internal negations to the primary outputs. Consequently, the type-selection domain of all non-output-layer gates is reduced from 16 to 8, while only output-layer gates must retain the full type set to absorb remaining negations.

THEOREM 4.1 (R TOPOLOGY-PRESERVING SIMPLIFICATION). *Given any Boolean circuit $C = (\mathcal{N} \cup I \cup O, E, \mathcal{T})$ over the full two-input gate-type library \mathcal{L} , there exists a functionally equivalent circuit $C' = (\mathcal{N} \cup I \cup O, E, \mathcal{T}')$ with the same node set and edge set such that*

every gate g outside the primary output layer satisfies

$$\mathcal{T}'(g) \in \mathcal{R},$$

where

$$\mathcal{R} = \{\text{XOR, OR, NAND, TRUE, } \neg A, \neg B, (\neg A) \vee B, A \vee (\neg B)\}.$$

Here, A and B denote the left and right input wires of a two-input gate, respectively. All gates in the primary output layer retain the full gate-type library \mathcal{L} . The circuit C' preserves the input–output behavior of C , i.e.,

$$\forall \mathbf{x} \in \{0, 1\}^n, \quad \text{Eval}(C)(\mathbf{x}) = \text{Eval}(C')(\mathbf{x}).$$

4.2 Backward Propagation Reduction

The second simplification exploits a complementary structural property of the circuit: certain gates are the sole consumers of one or both of their predecessor gates. Such “single-use” wiring enables local functional rewrites that preserve the I/O behavior and topology while reducing the admissible gate types for those positions.

If a gate g is the sole consumer of the output of one of its predecessor gates, then a logical negation at that predecessor can be reassigned without affecting any other part of the circuit. Consequently, the function at g can be replaced by an alternative gate type by pushing the negation upward to its fan-out = 1 predecessor, thereby reducing the number of gate types that g needs to consider.

For example, if an OR gate is driven by two predecessor gates that both have fan-out = 1, then it can be rewritten as a NAND gate by negating both of its inputs: $\text{OR}(a, b) = \text{NAND}(\neg a, \neg b)$. Since each predecessor gate drives only this OR gate, both can safely absorb the negation without affecting any other node in the circuit.

Definition 4.2 (S-Class Gate). A gate g is an S-Class gate if: (i) g is not a primary-input gate, and (ii) both of its input-driving predecessor gates have fan-out equal to 1.

Definition 4.3 (Z-Class Gate). A gate g is a Z-Class gate if: (i) g is not a primary-input gate, and (ii) exactly one of its input-driving predecessor gates has fan-out equal to 1.

THEOREM 4.4. *The sets of S-Class and Z-Class gates are disjoint.*

THEOREM 4.5 (ZS TOPOLOGY-PRESERVING SIMPLIFICATION). *Let $C = (\mathcal{N} \cup I \cup O, E, \mathcal{T})$ be a Boolean circuit over the full two-input gate-type library \mathcal{L} . Then there exists a functionally equivalent circuit $C' = (\mathcal{N} \cup I \cup O, E, \mathcal{T}')$ with the same node set and edge set such that*

$$\forall \mathbf{x} \in \{0, 1\}^n, \quad \text{Eval}(C)(\mathbf{x}) = \text{Eval}(C')(\mathbf{x}),$$

and the following hold:

- For every S-Class gate g , the assigned type satisfies $\mathcal{T}'(g) \in \mathcal{S} = \{\text{AND, NAND, XOR}\}$.
- For every Z-Class gate g , we refer to its two input wires as “left” and “right” merely following the netlist order, i.e., the first and second input wires in the Verilog description. If the unique fan-out = 1 predecessor drives the left (resp. right) input of g , then

$$\mathcal{T}'(g) \in \mathcal{Z}_{\text{left}} \text{ (resp. } \mathcal{Z}_{\text{right}}\text{),}$$

where $\mathcal{Z}_{\text{left}} = \{\text{XOR, AND, NAND, NOR, OR, } A\}$,

$\mathcal{Z}_{\text{right}} = \{\text{XOR, AND, NAND, NOR, OR, } B\}$.

- All remaining gates (those not in S-Class or Z-Class) retain the full library:

$$\mathcal{T}'(g) \in \mathcal{L}.$$

The ZS simplification preserves both the circuit topology and its end-to-end Boolean behavior.

4.3 Combined Reduction (ZSR)

The simplifications in Sections 4.1 and 4.2 exploit different circuit properties. The R simplification applies to all non-output-layer gates, while the ZS simplification applies only to Z and S-class gates. Since they target disjoint aspects of the circuit, the two are independent and can be applied in either order as preprocessing before SAT solving.

In practice, however, combining the two simplifications requires limited bookkeeping to preserve their intended effects. For example, when the ZS simplification is applied first, predecessor gates with fan-out = 1 must be explicitly recorded and forced to retain the full gate-type library. These gates must not be reassigned to the R-reduced class when the R simplification is subsequently applied. This coordination ensures that previously imposed gate-type restrictions are respected, so that the resulting circuit preserves the same input–output behavior.

We now describe a concrete preprocessing procedure that applies the ZS simplification followed by the R simplification.

Preprocessing procedure. Given a circuit $C = (\mathcal{N} \cup I \cup O, E, \mathcal{T})$, the attacker performs a single topological scan to obtain the fan-out of every gate and to identify the primary input and output layers. Gates are classified as follows:

- (1) If both immediate predecessors (fan-in gates) of a gate have fan-out = 1, restrict its type domain to \mathcal{S} .
- (2) ElseIf exactly one immediate predecessor has fan-out = 1, assign its type to $\mathcal{Z}_{\text{left}}$ or $\mathcal{Z}_{\text{right}}$, depending on whether the fan-out-1 predecessor drives the left or right input.
- (3) ElseIf the gate is neither in the primary output layer nor a predecessor of any \mathcal{S} or \mathcal{Z} type, restrict its type to \mathcal{R} .
- (4) All remaining gates retain the type \mathcal{L} , as they may be required to absorb negations propagated from upstream S/Z-gates or to handle any residual negations at the output layer.

The formal proofs of Theorems 4.1 and 4.5 are in Appendix A.

Resulting search-space partition. After this preprocessing step, gate-type assignments are decomposed as follows:

$$\mathcal{L}^{|\mathcal{N}|} \longrightarrow \mathcal{S}^{|\mathcal{N}_S|} \times \mathcal{Z}^{|\mathcal{N}_Z|} \times \mathcal{R}^{|\mathcal{N}_R|} \times \mathcal{L}^{|\mathcal{N}_F|},$$

where \mathcal{N}_S , \mathcal{N}_Z , and \mathcal{N}_R denote the sets of S-Class gates, Z-Class gates, and R-restricted gates, respectively. The set \mathcal{N}_F contains all remaining gates with unrestricted type domains (\mathcal{L}), including (i) primary output gates and (ii) non-S/Z-class gates that directly precede an S- or Z-class gate with fan-out 1. Table 1 summarizes the resulting gate categories and their admissible type sets.

Since $|\mathcal{S}| = 3$, $|\mathcal{Z}| = |\mathcal{Z}_{\text{left}}| = |\mathcal{Z}_{\text{right}}| = 6$, and $|\mathcal{R}| = 8$, these restrictions yield an exponential reduction in the size of the gate-type assignment space as a function of the number of gates.

Example. Figure 1 illustrates the combined gate-type domain reduction on a small circuit. Gate $g_4 \in \mathcal{N}_S$ is classified as an S-Class gate because both of its immediate predecessors g_0 and g_1 have fan-out = 1, and its admissible domain is therefore restricted

Gate category	Admissible type set
S-Class gates	\mathcal{S} (size = 3)
Z-Class gates	$\mathcal{Z}_{\text{left}}$ or $\mathcal{Z}_{\text{right}}$ (size = 6)
R-restricted gates	\mathcal{R} (size = 8)
Remaining gates	\mathcal{L} (size = 16)

Table 1: Resulting gate-type domains after applying the combined ZSR reduction.

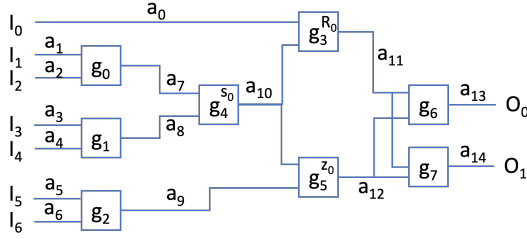


Figure 1: Example circuit annotated with S-Class gates (s_0), a Z-Class gate (z_0), and R-reduced gates (R_0). All remaining gates retain the full type library \mathcal{L} .

to \mathcal{S} . Gate $g_5 \in \mathcal{N}_Z$ is classified as a Z-Class gate since exactly one of its immediate predecessors (g_2) has fan-out = 1; assuming wire a_9 feeds its left input, its type domain is restricted to $\mathcal{Z}_{\text{left}}$. Gate $g_3 \in \mathcal{N}_R$ is assigned the reduced domain \mathcal{R} . All remaining gates (g_0, g_1, g_2, g_6 and g_7) belong to \mathcal{N}_F and retain the full gate-type library \mathcal{L} .

In this example, the naive search space of $16^8 \approx 4.3 \cdot 10^9$ gate-type assignments is reduced to $3^1 \cdot 6^1 \cdot 8^1 \cdot 16^5 \approx 1.5 \cdot 10^8$, an order of magnitude reduction induced by topology-based restrictions.

Remark 1. One may ask whether the restricted gate-type sets identified above can be further reduced to a basis consisting only of NAND or NOR gates. Such a reduction is not possible *without changing the topology*. NAND and NOR functional completeness relies on the ability to introduce additional gates and modify the circuit structure. In contrast, our recovery model requires the circuit topology to be preserved: each gate must remain a single node with its original fan-in, fan-out, and position. Under this constraint, each gate must be assigned a single primitive gate type rather than being implemented by a subcircuit.

5 SAT Encoding

Recovering an unknown gate-type assignment for a circuit with known topology can be reduced to deciding the satisfiability of a propositional formula that encodes (i) the public circuit topology τ , (ii) the selection of a gate type for each hidden gate, and (iii) the constraint that the instantiated circuit reproduces a set of observed input–output pairs $DI = \{(\mathbf{x}^{(i)}, \mathbf{z}^{(i)})\}$. We construct CNF formulas whose satisfying assignments are in 1-1 correspondence with gate-type assignments consistent with all observations.

We introduce four encoding primitives: $\text{EncodeCircuit}(\tau, T, DI)$, $\text{EncodeTwoCircuit}(\tau, T_1, T_2, DI)$, $\text{DiffConstr}(\tau, T_1, T_2, X)$, and

$\text{BlockCirc}(T_{\text{var}}, T_{\text{fixed}})$. Throughout, $\mathcal{L} = \{f_0, \dots, f_{15}\}$ denotes the full two-input Boolean gate library. Each gate g is associated with an admissible type domain $D(g) \subseteq \mathcal{L}$, specifying the set of Boolean functions that g may implement. In the baseline encoding, we take $D(g) = \mathcal{L}$ for all gates. As shown in Section 4, this domain can be restricted by preprocessing (e.g., R/S/Z simplification) to substantially reduce the SAT search space.

5.1 Variables and Basic Constraints

Type-selection variables. For every gate $g \in \mathcal{N}$ and every admissible type $t \in D(g)$, we introduce a Boolean selector variable $\text{Sel}_{g,t}$ (true iff gate g is assigned type t). Exactly-one selection per gate is enforced by the one-hot constraints $\Phi_{\text{onehot}}(\tau, T) :=$

$$\bigwedge_{g \in \mathcal{N}} \left(\bigvee_{t \in D(g)} \text{Sel}_{g,t} \wedge \bigwedge_{t, t' \in D(g), t \neq t'} (\neg \text{Sel}_{g,t} \vee \neg \text{Sel}_{g,t'}) \right).$$

Signal propagation. For every sample $(\mathbf{x}^{(i)}, \mathbf{z}^{(i)}) \in DI$ and every gate $g \in \mathcal{N}$, we introduce a signal variable $v_g^{(i)}$ representing the Boolean value on the output of g when the circuit is stimulated with $\mathbf{x}^{(i)}$. As in Definition 3.1, we use I and O to denote the sets of primary input and output nodes, respectively. Each input node $I_j \in I$ corresponds to one bit of $\mathbf{x}_j^{(i)}$, and each output node $O_h \in O$ is driven by a unique predecessor gate $\text{pred}(O_h)$ in the fixed topology. For a single sample, the constraints $\Phi_s(\mathbf{x}^{(i)}, \mathbf{z}^{(i)})$ are

$$\bigwedge_j^n (v_{I_j}^{(i)} = \mathbf{x}_j^{(i)}) \wedge \bigwedge_h^m (v_{\text{pred}(O_h)}^{(i)} = \mathbf{z}_h^{(i)}).$$

Each variable $v_{I_j}^{(i)}$ represents the Boolean signal on the j -th primary input wire when the circuit is evaluated on $\mathbf{x}^{(i)}$, and each $v_{O_h}^{(i)}$ represents the value observed on the h -th primary output wire. O_h is driven by a unique gate $\text{pred}(O_h)$ in the topology τ , ensuring that the output values $\mathbf{z}_h^{(i)}$ are correctly linked to the corresponding internal gate signals. Aggregating all samples yields:

$$\Phi_{\text{signals}}(\tau, DI) := \bigwedge_{(\mathbf{x}^{(i)}, \mathbf{z}^{(i)}) \in DI} \Phi_s(\mathbf{x}^{(i)}, \mathbf{z}^{(i)}).$$

Together, these variables define the Boolean search space over gate-type selections and signal assignments.

5.2 Circuit Encoding Primitives

We introduce the CNF encoding primitives used in the attack, which capture the functional correctness of symbolic gate-type assignments over observed input–output pairs DI . A two-circuit variant extends this encoding to jointly reason about two candidate assignments under a shared public topology.

All encodings are constructed by composing the variables and basic constraints introduced in Section 5.1. Concretely, each encoding combines the type-selection constraints Φ_{onehot} , the signal propagation constraints Φ_{signals} , and the gate semantics constraints defined below.

Gate semantics. For each gate $g \in \mathcal{N}$ with predecessors $u = \text{pred}_L(g)$ and $w = \text{pred}_R(g)$, the output signal is constrained to match the Boolean function selected by the gate-type variable:

$$\Phi_{\text{sem}}(g, T) := \bigwedge_{t \in D(g)} \left(\text{Sel}_{g,t} \Rightarrow (v_g \leftrightarrow f_t(v_u, v_w)) \right),$$

where $D(g) \subseteq \mathcal{L}$ denotes the admissible type domain of g . Each implication is compiled to CNF via standard Tseitin expansion over the truth table of f_t . Aggregating all gates yields

$$\Phi_{\text{semantics}}(\tau, T) := \bigwedge_{g \in \mathcal{N}} \Phi_{\text{semantics}}(g, T).$$

Single-circuit encoding. Given a public topology τ and a symbolic gate-type assignment T , the encoding $\text{EncodeCircuit}(\tau, T, DI) :=$

$$\Phi_{\text{onehot}}(\tau, T) \wedge \Phi_{\text{signals}}(\tau, DI) \wedge \Phi_{\text{semantics}}(\tau, T)$$

enforces that the instantiated circuit reproduces all observed input-output pairs in DI . Any satisfying assignment yields a concrete gate-type assignment consistent with the observations.

Two-circuit encoding. To compare two candidate assignments under identical observed behavior, we construct two disjoint copies of the single-circuit encoding under the same topology. Given T_1 and T_2 , we define $\text{EncodeTwoCircuit}(\tau, T_1, T_2, DI) :=$

$$\bigwedge_{j \in \{1, 2\}} \text{EncodeCircuit}(\tau, T_j, DI),$$

where all type-selection and signal variables are namespace-isolated across the two copies. Any satisfying assignment yields two distinct gate-type assignments that are consistent with all observations in DI . A discriminating input separating the two assignments is enforced by an additional constraint introduced in Section 5.3.

Optional domain restriction. Both encodings can accept restricted domains $D(g)$ derived from topology-based preprocessing (§4).

5.3 Encoding of Discriminating Inputs

The goal of this encoding is to identify a discriminating input (a primary-input vector) that causes two gate-type assignments to produce different primary outputs. This primitive serves as the bridge between the two-circuit encoding in Section 5.2 and the iterative search procedure: given two candidate circuits that are both consistent with the known input-output set DI , it searches for a new input vector that can distinguish between them.

We capture this with the CNF primitive $\text{DiffConstr}(\tau, T_1, T_2, X)$, where τ is the public circuit topology, T_1 and T_2 are two (possibly symbolic) gate-type assignments, and X is a vector of primary-input Boolean variables. We denote by $v_{O_t,1}^{(X)}$ and $v_{O_t,2}^{(X)}$ the primary-output signal variables corresponding to input X in the two circuit copies. We encode that X distinguishes T_1 and T_2 by asserting that at least one primary-output bit differs:

$$\text{DiffConstr}(\tau, T_1, T_2, X) := \bigvee_{\ell} (v_{O_t,1}^{(X)} \oplus v_{O_t,2}^{(X)}).$$

$\text{DiffConstr}(\tau, T_1, T_2, X)$ is satisfiable iff there is an input X on which the two instantiated circuits produce different primary outputs. It is the logical mechanism for discovering new oracle queries.

5.4 Blocking Concrete Gate-type Assignments

The fourth primitive, BlockCirc , excludes a concrete gate-type assignment from all future satisfying assignments by enforcing that any symbolic gate-type assignment must differ from that concrete assignment on at least one gate.

Algorithm 1 High-level Baseline SAT-based Function Recovery Algorithm

Require: Circuit Topology τ , oracle $\text{Oracle}_f(\cdot)$
Ensure: Equivalent gate-type assignment \mathcal{T}

- 1: $DI \leftarrow \emptyset$
- 2: **while** True **do**
- 3: Solve for two gate-type assignments $\mathcal{T}_1, \mathcal{T}_2$, and an input vector \mathbf{x} , s.t. $\mathcal{T}_1, \mathcal{T}_2$ are consistent with all pairs in DI , yet produce different outputs on input \mathbf{x} .
- 4: **if** $(\mathcal{T}_1, \mathcal{T}_2, \mathbf{x})$ exists **then**
- 5: Query $\text{Oracle}_f(\mathbf{x})$ to obtain output vector \mathbf{z}
- 6: Update $DI \leftarrow DI \cup \{(\mathbf{x}, \mathbf{z})\}$
- 7: Block gate-type assignments inconsistent with (\mathbf{x}, \mathbf{z})
- 8: **else break**
- 9: **end if**
- 10: **end while**
- 11: Obtain \mathcal{T} s.t. the corresponding circuit satisfies all pairs $\{(\mathbf{x}, \mathbf{z})\} \in DI$
- 12: **return** \mathcal{T}

Let T denote the symbolic gate-type assignment and \mathcal{T} a concrete assignment that maps each gate g to a specific type $\mathcal{T}(g)$. The blocking clause that forbids \mathcal{T} is

$$\text{BlockCirc}(T, \mathcal{T}) := \bigvee_{g \in \mathcal{N}} \neg \text{Sel}_{g, \mathcal{T}(g)},$$

where $\text{Sel}_{g, \mathcal{T}(g)}$ are the one-hot selector variables introduced in Section 5.1. This disjunction asserts that any future model must change the type of at least one gate w.r.t. \mathcal{T} .

6 Baseline Attack

In this section, we establish a SAT-based baseline for Threat Model A by adapting the decamouflage framework of El Massad et al. [1]. In their original setting, the focus is on scenarios in which only a small subset of gates is obfuscated, and the attacker leverages a discriminating input set together with SAT solving to pinpoint those hidden positions. In contrast, our GH threat model conceals the type of every gate behind uniform encodings, substantially enlarging the search space. We generalize the same counterexample guided strategy to this more demanding scenario.

The central strategy of our attack involves constructing a discriminating input-output (I/O) pair set $DI = \{(\mathbf{x}, \mathbf{z})\}$, where each pair (\mathbf{x}, \mathbf{z}) consists of an input vector and the corresponding output obtained by oracle query $\text{Oracle}_f(\mathbf{x})$. This set is iteratively expanded to eliminate incorrect candidate gate-type assignments.

The key idea of Algorithm 1 (lines 3–8) is to iteratively identify inputs that distinguish between conflicting candidate solutions: in line 3, two candidate gate-type assignments ($\mathcal{T}_1, \mathcal{T}_2$) that are consistent with all observed input-output pairs currently in DI are located. We then search for an input vector \mathbf{x} on which these two candidates produce different outputs. If such two gate-type assignments and discriminating input exist (lines 4–7), the oracle $\text{Oracle}_f(\cdot)$ is queried to obtain the output \mathbf{z} , and the new pair (\mathbf{x}, \mathbf{z}) is appended to DI . Any gate-type assignment inconsistent with this new observation is then blocked (line 7). This process repeats until no additional distinguishing input can be found (line 8), at which point the

Algorithm 2 Intuition of the Enhanced SAT-based Function Recovery Algorithm

Require: Circuit topology τ , oracle $\text{Oracle}_f(\cdot)$
Ensure: Equivalent gate-type assignment \mathcal{T}

- 1: Classify all gates in τ and initialize per-gate type domains using the Simplification Theorems
- 2: $DI \leftarrow \emptyset$
- 3: **while** true **do** ▷ repeat until DI is complete
- 4: Obtain a gate-type assignment \mathcal{T}_1 that satisfies all pairs in DI
- 5: **while** another gate-type assignment satisfies DI **do**
- 6: Obtain a different assignment \mathcal{T}_2 that satisfies DI
- 7: Obtain a discriminating input \mathbf{x} between \mathcal{T}_1 and \mathcal{T}_2
- 8: **if** such \mathbf{x} exists **then**
- 9: Query $\text{Oracle}_f(\mathbf{x})$ for output \mathbf{z}
- 10: $DI \leftarrow DI \cup \{(\mathbf{x}, \mathbf{z})\}$
- 11: Block any gate-type assignment that mispredicts \mathbf{x}
- 12: **break** inner while
- 13: **else**
- 14: Block \mathcal{T}_2 within the current inner loop
- 15: **continue**
- 16: **end if**
- 17: **end while**
- 18: **if** no new assignment exists **then** **break** outer while
- 19: **end while**
- 20: **return** \mathcal{T}_1

discriminating set DI is said to be *complete*. Finally, as shown in line 11, a gate-type assignment \mathcal{T} that satisfies all pairs in the complete DI is extracted as the recovered function. Formally, such a complete discriminating set guarantees that any two assignments consistent with all $(\mathbf{x}, \mathbf{z}) \in DI$ are functionally indistinguishable over the entire input space. For a formal proof of completeness and correctness, see [1]. To complement the high-level description, the detailed steps are in Algorithm 3 in Appendix B.

7 Our Optimized Attack

We present an optimized SAT-based function-recovery attack under Threat Model A. While the baseline approach encodes symbolic variables representing two candidate gate-type assignments together with a symbolic discriminating input into a single, monolithic SAT instance, our optimized attack decomposes each recovery iteration into a sequence of smaller and more focused SAT queries. This decomposition separates the tasks of identifying candidate assignments and searching for a discriminating input, thereby reducing the complexity of each individual SAT instance.

In addition, our optimized attack incorporates the topology preserving simplification theorems from Section 4 as a preprocessing step. These simplifications restrict the admissible gate-type domain of each gate based solely on the public circuit topology. The same optimization principles extend directly to Threat Model B, the optimized attack for Threat Model B is described in detail in Section 8.

In the baseline algorithm, the solver must jointly find a discriminating input and two functionally distinct gate-type assignments, causing the constraint space to grow quickly as more input-output

pairs are added to DI . To reduce this complexity, we adopt a divide-and-conquer strategy: the solver first generates candidate gate-type assignments consistent with all observed input-output pairs in DI . A separate SAT query then searches for a distinguishing input between any two candidates. If no such input exists for the selected pair, indicating functional equivalence between them, we return to sampling a new candidate assignment.

Algorithm 2 summarizes the optimized SAT-based function recovery procedure under Threat Model A. The algorithm first classifies all gates and applies the Simplification Theorems to initialize per-gate type domains (line 1). It then iteratively maintains a discriminating-input set, starting empty (line 2). In each iteration of the outer loop (line 3), the solver obtains a gate-type assignment consistent with all observed input-output pairs (line 4). The inner loop (line 5) repeatedly generates additional assignments that also satisfy the current discriminating set (line 6) and attempts to construct a discriminating input separating them from the reference assignment (line 7). When such an input is found, the oracle is queried (line 9), the discriminating set is updated, and all assignments inconsistent with the new evidence are globally blocked (line 11), after which the search restarts. If no discriminating input exists for the current candidate, that candidate is blocked within the current inner-loop iteration (line 14) so that the search may continue, although it may reappear once the outer loop restarts. When no further candidates remain in the inner loop, the algorithm concludes the enumeration phase.

One potential concern is that the inner enumeration loop may not terminate efficiently when the number of satisfiable gate-type assignments is large. To address this, we implement an early termination mechanism. Instead of exhaustively enumerating all gate-type assignments consistent with the current discriminating set, the algorithm collects up to N_{\max} such assignments and then issues a monolithic SAT query with the first assignment fixed to \mathcal{T}_1 . If this query is UNSAT, it certifies that no further distinguishing input exists, and the enumeration phase terminates soundly. For simplicity, we fix $N_{\max} = 3$ in all experiments. Although this choice is not minimal, it is sufficient in practice to prevent excessive iterations of the inner loop and to demonstrate the effectiveness of our approach, without affecting the qualitative conclusions.

To complement the high-level intuition, Algorithm 4 in Appendix B provides the full SAT-based formulation of our optimized function-recovery procedure, including the explicit encodings and blocking constraints. The encoding follows directly from Algorithm 2.

8 Extended Attack under Hidden Inputs

We now extend the optimized attack framework to Threat Model B, where only a subset of the circuit inputs is controllable by the adversary. In this setting, the adversary no longer observes the full input-output behavior of the target circuit, but instead queries the oracle on inputs of the form \mathbf{x} , receiving outputs corresponding to $\text{Eval}(C)(\mathbf{x}, \mathbf{y})$ for an unknown but fixed \mathbf{y} .

From the attacker's perspective, this hidden input introduces ambiguity: multiple gate-type assignments that are distinguishable under full input control may become observationally equivalent

once part of the input is fixed and concealed. As a result, the recovery task must account for both structural uncertainty (the hidden gate types) and input uncertainty induced by the unknown \mathbf{y} .

To address this challenge, we adapt the SAT-based recovery procedure to jointly reason about gate-type assignments and the hidden input. The core attack structure remains counterexample-guided, but the SAT encodings and discriminating-input search are modified to incorporate \mathbf{y} as an additional unknown that must remain consistent across all oracle queries. We detail the resulting changes to the SAT encoding and recovery procedure, and present the extended attack algorithm in the remainder of this section.

To support joint recovery of \mathcal{T} and \mathbf{y} , we extend the SAT-based formulation by introducing Boolean variables corresponding to each bit of \mathbf{y} . They are incorporated into the same encoding framework as the one-hot gate-type selectors used to model \mathcal{T} , allowing the solver to reason jointly about hidden gates and inputs.

Our attack follows the same counterexample-guided refinement structure as in Threat Model A, but now searches the joint space $\mathcal{L}^k \times \{0, 1\}^{n'}$. Since all topology-preserving Simplification Theorems remain applicable, the same per-gate domain reductions are applied before each SAT invocation, yielding a significantly smaller combined search space. In each iteration, the solver performs:

- (1) **Candidate generation:** Solve the SAT instance to obtain a candidate pair (\mathcal{T}_1, Y_1) that satisfies all constraints induced by the current discriminating set DI .
- (2) **Enumeration of alternatives:** Add a blocking clause for (\mathcal{T}_1, Y_1) and re-solve for a distinct pair (\mathcal{T}_2, Y_2) .
- (3) **Discriminating input search:** Fix both candidate pairs (\mathcal{T}_1, Y_1) and (\mathcal{T}_2, Y_2) and solve for an input vector $\mathbf{x} \in \{0, 1\}^n$ such that $\text{Eval}((\tau, \mathcal{T}_1))(\mathbf{x}, Y_1) \neq \text{Eval}((\tau, \mathcal{T}_2))(\mathbf{x}, Y_2)$. If such an \mathbf{x} exists, the corresponding oracle output is queried and the resulting pair (\mathbf{x}, \mathbf{z}) is added to DI .

The discriminating set DI is complete once no additional candidate pair satisfies the accumulated constraints and can be distinguished from (\mathcal{T}_1, Y_1) by any attacker-controlled input. At this point, all remaining candidate pairs are functionally equivalent with respect to the attacker-controlled input domain.

Since the hidden input vector \mathbf{y} is fixed across all oracle queries, each discovered discriminating input remains valid and eliminates at least one candidate. Once the discriminating set DI is complete, a final SAT query extracts a pair (\mathcal{T}, Y) that is *functionally equivalent* to the true circuit over the controllable input domain.

9 Benchmark Circuits

All evaluated circuits are combinational Boolean circuits, consistent with the circuit model assumed by garbled-circuit protocols. This restriction allows us to isolate and study the function-recovery problem induced by gate hiding, without introducing orthogonal challenges such as sequential state reconstruction. Point functions, which represent an extreme case for function recovery, are analyzed separately in a dedicated section.

To match the gate-level structure assumed in gate-hiding protocols, we synthesize all designs using Synopsys Design Compiler with a complete two-input Boolean gate library of size sixteen. This library corresponds to the most general two-input Boolean gate

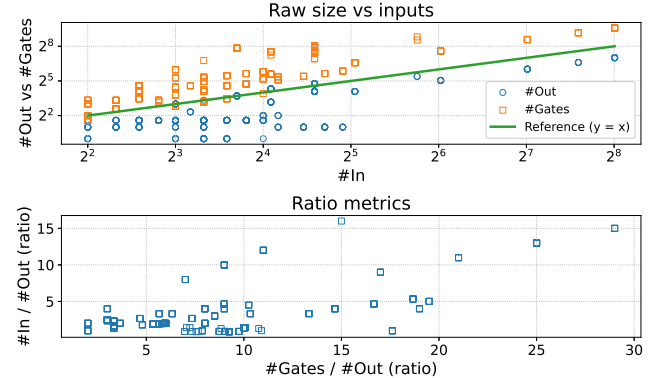


Figure 2: Circuit Complexity of the Evaluated Benchmarks. The top plot shows outputs and gates versus inputs; the bottom plot summarizes complexity using gate-to-output and input-to-output ratios.

model used in gate-hiding constructions and induces maximal gate-type uncertainty for function recovery attacks.

The benchmark set comprises three classes of combinational circuits. Figure 2 summarizes the distribution of circuit sizes across the evaluation suite. We describe each class in detail below.

- (1) **ISCAS Benchmarks.** We include standard benchmarks from ISCAS'89. Following [1], sequential circuits are converted to combinational form by unrolling one cycle and replacing each flip-flop with a primary input. High fan-in gates are further decomposed into cascaded two-input gates to ensure compatibility with the gate-hiding model.
- (2) **2PC Cryptographic Circuits.** We evaluate three families of commonly used two-party computation circuits, including adders, comparators, and Hamming-distance designs. Each family is synthesized at multiple input sizes to assess scalability and structural variation.
- (3) **Sensor-Fusion MPC Circuits.** To assess MPC-specific logic, we include compact combinational circuits derived from the privacy-preserving sensor-fusion algorithms of [4]. The number of input sensors ranges from 3 to 19. Although modest in absolute size, these circuits preserve the algorithmic structure and data-flow dependencies of the original designs.

Comparison with Decamouflaging Benchmarks. Prior SAT-based decamouflaging studies typically considered partial camouflage, in which only a small fraction of gates is hidden. For example, El Massad et al. [1] followed the setting of [15], camouflaging fewer than 10% of the gates in large ISCAS circuits and modeling each camouflaged gate with two or three possible identities. Their largest evaluated configuration corresponds to a search space of approximately 3^{350} . In contrast, our benchmarks include circuits with up to 768 gates, where every gate may realize any of sixteen two-input Boolean functions, yielding an effective search space on the order of 16^{768} . Gate count alone is not a complete indicator of recovery difficulty across these settings. Even moderate-sized circuits under our GH model can induce substantially larger uncertainty than much larger circuits subject to partial camouflage.

10 Experimental Evaluation

10.1 Experimental Setup

We evaluate SAT-based function recovery attacks under two distinct threat models: (1) Model A and (2) Model B. Each model is tested with and without the proposed simplification theorem, enabling a direct comparison of its effect on search-space reduction and solver runtime. Algorithm 1 serves as the baseline.

All attacks are executed on AWS EC2 r7i.xlarge instances (4 vCPUs, 32 GiB RAM), with a 24-hour time budget per attack. We report only circuits that are successfully recovered within this time window. The implementation is written in Python 3 and uses Glucose3 via PySAT for SAT solving. We perform one run per circuit, which may reflect conservative runtime and discriminating-set sizes. This setup is sufficient to identify dominant trends and demonstrate the practical effectiveness of the proposed attacks.

10.2 Experimental Results

To facilitate comparison with prior work, we first evaluate our attack on selected ISCAS'89 benchmark circuits under Model A. The results are summarized in Table 2. For each circuit, the table reports its number of primary inputs and outputs, total gate count (excluding NOT gates), and the number of S-Class and Z-Class gates. We evaluate four configurations: our optimized algorithm with and without the Simplification Theorems (Ours+Simpl and Ours) and the monolithic baseline under the same two settings (Baseline+Simpl and Baseline). Each entry lists the recovery runtime in seconds, followed by the size of the resulting discriminating set in parentheses. Across the ISCAS'89 benchmark circuits, the optimized approach significantly outperforms the baseline. The improvement is most pronounced when the Simplification Theorems are enabled. For example, on circuit s298, our algorithm with R simplification completes function recovery in 51.73 s, whereas the baseline requires 857.32 s, yielding a speedup of approximately 16.6x. The two approaches recover complete discriminating input sets of sizes 103 and 94, respectively.

Figure 3 reports the log-scale recovery time for four representative MPC-style functions, namely Adder, Comparator, Hamming Distance, and SS (the Schmid–Schossmaier interval-fusion algorithm used in fault-tolerant sensor fusion [4]), under both Model A and Model B. Each subplot corresponds to a fixed MPC functionality instantiated with different input sizes. All functions are evaluated under the same four solver configurations as in Table 2: Ours + Simpl, Ours, Baseline+Simpl, and Baseline. As a concrete example, for a 14-bit input Hamming distance function, the optimized algorithm with ZSR simplification (OURS+ZSR) successfully recovers the function within 20.50 s, issuing 23 oracle queries. In contrast, the baseline algorithm without simplification requires 3251.64 s and 22 oracle queries, corresponding to a speedup of approximately 159x.

For several larger instances, missing data points indicate that the corresponding algorithm did not complete within the 24-hour time budget. In contrast, Ours+Simpl successfully handles all tested input sizes, while Ours covers most of the range. Both baseline configurations encounter timeout failures more frequently as the circuit size increases. Although the fully optimized attack does not

always achieve the lowest recovery time for small circuits, the performance gap between different approaches widens with increasing circuit size, and Ours+Simpl consistently becomes the most efficient strategy for larger instances. This behavior is expected, as the proposed optimizations primarily reduce the search space and constraint complexity, whose benefits become more pronounced at scale. Among the four functions, the Adder benchmark exhibits the most stable and regular trend across input sizes. Compared to the other functions, the performance gap between different solver configurations is less pronounced, and the benefit of the optimized attack is correspondingly smaller. This behavior is consistent with the relatively simple and regular structure of adder circuits.

Across all evaluated circuits, the discriminating input set sizes remain comparable across different optimization stages and within the same order of magnitude, indicating that the observed runtime improvements are not attributable to reduced oracle queries. As shown in the second subfigure of Fig. 6, the number of queries is typically small, remaining below $1025 \approx 2^{10}$ even for circuits with a large gate-to-output ratio.

Figure 4 isolates the effect of gate-type simplification by comparing, for each benchmark circuit, the recovery runtime with simplification (x-axis) against the runtime without simplification (y-axis), under Models A and B. Each circuit contributes up to two points, one for the baseline and one for our optimized algorithm, so the plot evaluates the simplification step consistently across algorithms. Points above the diagonal indicate a speedup from simplification, while points below indicate a slowdown. Cases that succeed only with simplification have no corresponding no-simplification runtime and are therefore omitted; their counts are reported in the in-plot annotations. Overall, the concentration of points above the diagonal shows that simplification yields broad and consistent runtime reductions in both models.

We further compare our re-implementation and generalization of the baseline monolithic approach with our optimized attack. Figure 5 plots the recovery time of the two algorithms on the same set of instances under Model A and Model B, where each point corresponds to one circuit instance. The diagonal line indicates equal runtime for both approaches. Points below the diagonal therefore represent instances where the optimized attack is slower. Under both threat models, the majority of instances lie above the diagonal, indicating that the optimized algorithm consistently achieves lower recovery time than the baseline. Moreover, many points deviate substantially from the diagonal, reflecting speedups of multiple orders of magnitude on a logarithmic scale. The summary statistics further confirm this trend: for most instances solved by both algorithms, the optimized attack is faster, and it additionally succeeds on several instances where the baseline fails to terminate within the time limit.

In summary, our experiments show that the proposed incremental SAT attack substantially outperforms the baseline in recovery time on most tested circuits, with further gains enabled by topology-preserving simplifications. The attack is effective under both threat models and requires only modest oracle interaction, supporting its practical applicability.

Circuit	#In	#Out	#Gates	#S	#Z	Ours+Simpl	Ours	Baseline+Simpl	Baseline
s27a	7	3	8	0	0	R, 0.01 (12)	0.06 (18)	R, 0.00 (16)	0.25 (14)
s298	17	20	125	14	10	R, 51.73 (103)	357.64 (97)	R, 119.88 (85)	857.32 (94)
s344	24	17	109	1	8	R, 688.71 (68)	1,554.40 (77)	R, 1,311.27 (58)	3,300.54 (63)
s349	24	17	112	1	8	R, 821.96 (69)	1,226.76 (72)	R, 867.75 (68)	3,550.64 (82)
s382	24	27	148	8	25	ZSR, 816.39 (76)	3,299.32 (68)	-	-
s386	13	13	188	6	5	R, 273.93 (257)	1,743.41 (239)	ZSR, 758.41 (268)	-
s400	24	27	158	9	27	ZS, 2,509.63 (81)	3,328.19 (86)	-	-
s444	24	27	171	5	22	R, 1,179.96 (66)	6,674.82 (93)	-	-

* The attack runtime is reported in seconds, and the size of the discriminating set is shown in parentheses. “-” indicates time-out.

Table 2: Performance Comparison on ISCAS89 Benchmarks under Model A.

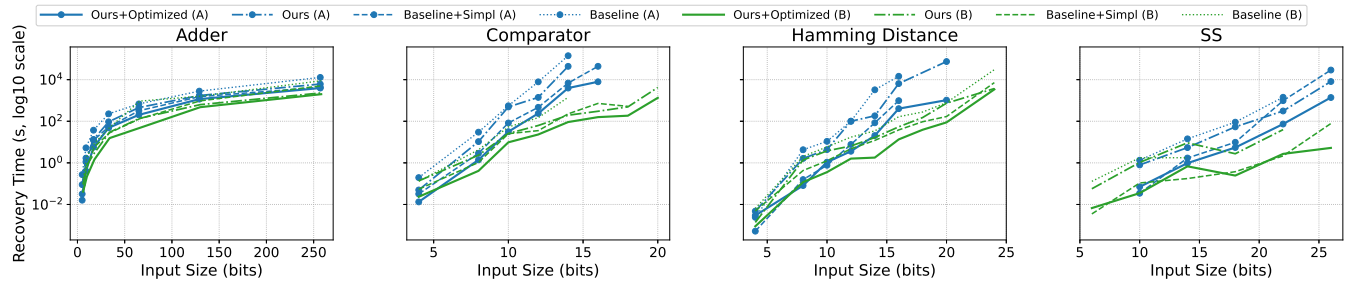


Figure 3: Log-scale recovery runtime on representative MPC functions. Each subplot reports the recovery time as a function of input size for a fixed MPC functionality (Adder, Comparator, Hamming Distance, and SS). Results are shown under both threat models, with Model A in blue and Model B in green, and for four solver configurations: Ours+Simpl, Ours, Baseline+Simpl, and Baseline. The y-axis is plotted on a logarithmic scale.

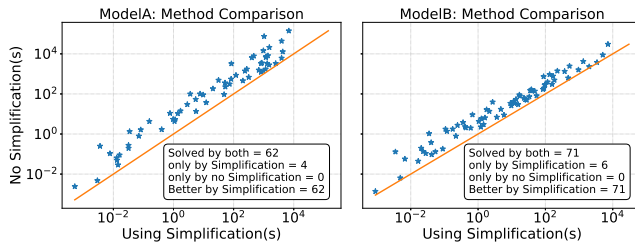


Figure 4: Overall Impact of Simplifications

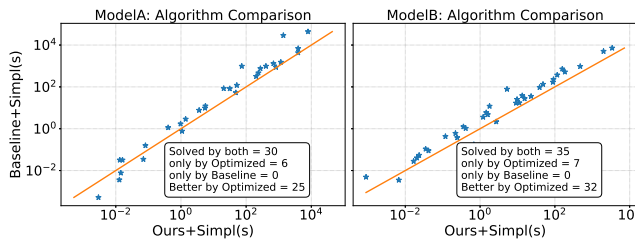


Figure 5: Impact of Baseline vs Optimized Algorithm

10.2.1 Circuit Complexity and Discriminating Inputs. Because the recovery process relies on discriminating inputs to separate candidate gate-type assignments, we examine how different circuit characteristics relate to the number of discriminating inputs required.

Figure 6 reports the number of discriminating inputs for all circuit instances solved within the time limit.

We observe that the number of primary inputs alone is not a reliable indicator of circuit complexity, as it shows little correlation with the number of discriminating inputs. In contrast, the data exhibits a clear increasing trend with respect to the ratio between the number of gates and outputs, which better reflects the structural complexity of the circuit. The rightmost subfigures further show that both recovery time and the number of discriminating inputs grow with this ratio, indicating its relevance to both oracle interaction and solver runtime.

Overall, the number of discriminating inputs required for complete recovery varies across benchmarks but remains well below the theoretical input space. Even in the most challenging instances, fewer than 2^{10} discriminating inputs suffice to recover circuits with 18 primary inputs, compared to $2^{18} \approx 2.6 \times 10^5$ possible input combinations. This observation is consistent with the fact that circuit topology significantly constrains the space of valid gate-type assignments, enabling recovery with far fewer oracle queries than exhaustive enumeration.

11 Testing the Limits: Point Functions

Point functions provide a natural stress test for function recovery attacks. They output one on exactly a single input out of $2^{\#In}$, and zero on all the others. In this section, we assume that the attacker

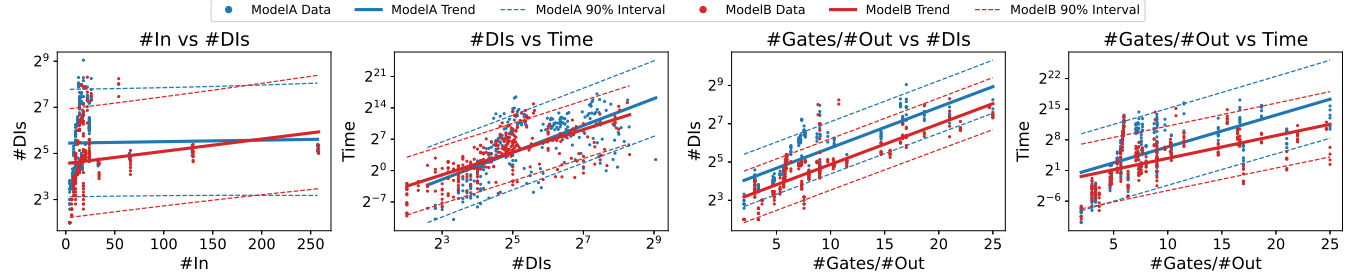


Figure 6: Scaling of discriminating inputs and solver time with circuit complexity for Models A and B. Each panel shows data (points), log-domain linear trends (solid), and 90% prediction intervals (dashed), across four views: (a) #In vs #DIs (\log_2 y); (b) #DIs vs time (\log_2 – \log_2); (c) #Gates/#Out vs #DIs (\log_2 y); (d) #Gates/#Out vs time (\log_2 y).

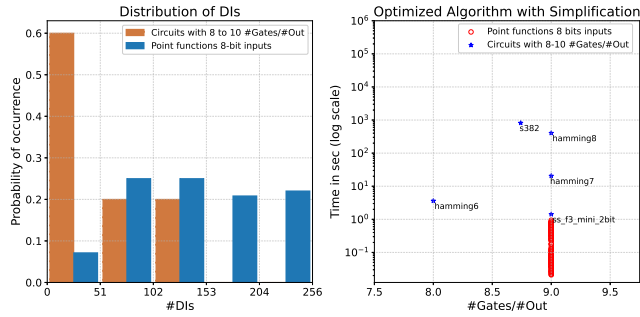


Figure 7: Comparing 8-bits Point Functions with Circuits having similar #Gates/#Out ratio

does not know whether the target circuit implements a point function. Consequently, from an oracle-only perspective, an adversary cannot certify that a circuit implements a point function without querying the entire input space, since any unqueried input may still yield output one.

In our setting, the attacker has access to the circuit topology. In some instances, a small number of oracle queries suffices to recover the target function. At that point, the attacker can certify that no input distinguishes any pair of remaining gate-type assignments, and hence that they are functionally equivalent. This, however, does not improve the worst-case number of oracle queries, which can still be $2^{\#In}$. Knowing the circuit topology constrains the set of realizable functions, but does not give any bias toward the location of the unique triggering input. Moreover, since we allow a full gate-type set, the same circuit topology can be used to represent any point function of the same input size.

To study this boundary case, we exhaustively evaluated all 8-bit point functions and compared them against circuits with a similar #Gates/#Out ratio. The left side of Figure 7 shows that point functions can require more discriminating inputs than other circuits of comparable structural complexity, consistent with the oracle-query difficulty discussed above. In contrast, the right side of the figure shows that the total recovery time for point functions is often smaller, due to their concise circuit structure.

12 Related Work

Semi-private function evaluation. Paus et al.[14] present a semi-private function evaluation (SPFE) scheme based on privately programmable blocks (PPBs) that supports secure computation of class-specified functions while exposing circuit topology. In their paper, Yao's garbled circuits scheme is regarded as a semi-private function evaluation. Daniel et al.[2] develop a framework for SPFE and show the practicality by developing a car insurance application. The core idea is to use universal circuits for the private part of the function, while the other part remains public. Vladimir Kolesnikov [7] proposed a semi-private function evaluation (semi-PFE) scheme based on a special type of circuit that can represent a pre-defined set of functions. While the proposed scheme ensures that the evaluator cannot distinguish which specific function was evaluated among a publicly known set S , it does not protect the privacy of the function set itself. Since all possible functions and their topologies are explicitly known to the evaluator, the scheme inherently leaks the structure and behavior of every function in S .

GH Garbled Circuits. Rosulek proposed two GH schemes in [16], both of which achieve effective gate-hiding but incur significant computational overhead due to additional hashing and insertion operations. Compared to Free-XOR-enabled, non-gate-hiding schemes, these constructions require increased storage, communication, and evaluation effort, particularly in circuits with a high density of XOR gates. To enhance the efficiency of GH garbled circuits, Lin et al. [11] introduced a skipping scheme that leverages prime implicants to eliminate redundant computation paths. While this method reduces evaluation cost, the process of identifying skippable wire pairs and computing prime implicants remains computationally intensive and time-consuming. In a major advancement, Rosulek et al. [17] broke the long-standing communication lower bound in Boolean garbled circuits by reducing the communication cost of a 2-input gate to just $1.5k + O(1)$ bits (for security parameter k), establishing a new minimal bound. Notably, this encoding applies uniformly to all 16 possible 2-input Boolean gates.

SAT Solver for Cryptanalysis Massacci and Marraro [12] introduced Logical Cryptanalysis for cryptographic algorithms. It converts cryptanalysis problems into Boolean satisfiability problems (SAT) to analyze the security of cryptographic algorithms, such as DES. Logical Cryptanalysis includes encoding the algorithm, adding constraints corresponding to plaintext/ciphertext pairs, and

applying SAT solvers. While the paper demonstrated the potential of applying SAT to cryptanalysis algorithms, its scalability, its practical applicability was limited by the ability of SAT solvers at the time to process practical circuits.

Only 15 years later, El Massad et al. [1] introduced an effective SAT-based attack for reverse engineering camouflaged integrated circuits (ICs), formally defining the decamouflaging problem. Their approach recovers camouflaged gate configurations in minutes by identifying small sets of discriminating input patterns. The effectiveness of this method continues to be explored in subsequent work [25]. Our Threat Model A can be viewed as a generalized extension of the decamouflaging setting, where all gates are assumed to be camouflaged and each gate may implement an arbitrary 2-input Boolean function. This generalization results in a substantially larger search space than that encountered in traditional IC camouflaging scenarios.

SAT-based Attacks on Logic Locking. Logic locking (or logic encryption) is a hardware security technique that modifies the functionality of a circuit such that it behaves correctly only when a secret key is applied, thereby preventing unauthorized use or reverse engineering of integrated circuits. Subramanyan et al. [20] introduced the first SAT-based attack capable of defeating all known combinational logic locking schemes at the time. Their approach efficiently recovers the correct key by iteratively pruning incorrect key candidates using distinguishing input patterns. Hai et al. [28] extended this attack methodology to cyclic logic locking, challenging the prevailing assumption that SAT-based attacks are ineffective in the presence of cycles. Their CycSAT technique introduces additional constraints at potential feedback locations to manage cycles. Shen et al. [19] proposed a SAT-based bit-flipping attack targeting logic locking schemes that combine traditional XOR/XNOR locking with SAT-hard structures. Their method flips each key bit individually, using the number of resulting distinguishing inputs to partition the key bits into SAT-resolvable and SAT-proof subsets. The SAT-resolvable subkey is recovered using a conventional solver, while the SAT-proof subkey is inferred via a bypass mechanism. After the introduction of SAT attacks on logic locking schemes, many SAT resilient schemes have been proposed. Both SARLock [24] and Anti-SAT [22] deliberately force a SAT solver to require exponentially more iterations by ensuring that any wrong key yields only one (for SARLock) or at most two (for Anti-SAT) distinguishing outputs. However, by driving the error rate under incorrect keys to near zero, both schemes become inherently susceptible to bypass attack [23].

13 Limitations of this work

Our algorithm does not aim to minimize the size of the discriminating set. Although multiple complete discriminating sets may exist, the solver only discovers one distinguishing input per iteration, which is enough to separate one pair of gate-type assignments. Our goal is not to optimize the discriminating set itself, but rather to accelerate each solving step, meaning the time required to obtain a single distinguishing input. This acceleration comes from reducing the candidate search space and shrinking the SAT constraints used in each iteration. Therefore, for circuits that have a large discriminating set, the attacker may encounter this larger set during the

attack process, and the total time required for function recovery can become significantly larger. Section 11 shows one such example, namely point functions. Identifying a minimum discriminating set during the attack remains future work.

Given this limitation, an effective mitigation is to incorporate point-function-like structures into the circuit to intentionally enlarge the discriminating set. Another possible direction is to add constraints in each iteration to help identify a discriminating input that can distinguish more than two gate-type assignments, which could reduce the size of the discriminating set found during the attack.

In our experiments, we observed that the scalability of the attack is influenced by available computational resources, in particular the number of virtual CPUs and the amount of memory. For this reason, we do not aim to determine the largest circuit that can be attacked, as the attack will eventually terminate given sufficient time and resources, although the exact runtime is unknown. Our evaluation focuses instead on demonstrating the effectiveness of our optimization techniques in accelerating the attack.

Function recovery under Model B, where the attacker must infer both the circuit logic and the unknown input vector, can be influenced by the specific value of the hidden input y . In our experiments, we randomly selected a value of y . Since our method is designed to recover arbitrary fixed y , we do not characterize how different choices of y affect solver performance, as this is tightly coupled to the functionality of each circuit. Exploring the interaction between circuit functionality, hidden inputs, and solver complexity is a valuable direction for future work.

14 Countermeasures and Conclusion

In this work, we demonstrate how to exploit a largely overlooked leakage channel in gate-hiding garbled circuits: the circuit topology. We show that this structural information can be leveraged to efficiently recover the functionality of a hidden circuit using only a small number of oracle queries. Our proposed simplification theorem and incremental SAT-solving strategy significantly accelerate function recovery compared to the baseline attack.

Our findings serve as a cautionary note, highlighting the need for careful consideration before the widespread adoption of gate-hiding garbled circuit techniques. As a potential countermeasure, we suggest introducing circuit-level redundancy, such as additional gates, expanded input domains, and strategically placed constant gates, which can artificially inflate the complexity of the underlying SAT problem and hinder efficient function recovery. Reduce the number of Z-Class and S-Class gates in the circuit constitutes another mitigation strategy, as it limits the effectiveness of ZS-based simplification.

Although our discussion focuses on a two party scenario in which one participant holds a private function and the other holds private inputs, our framework extends seamlessly to multiparty settings, where one party has the secret function and garbles the gates, and the other parties contribute data to be evaluated in the circuit [4]. Threat model B is an example of this scenario, where the second input might come from a different party than A.

15 Acknowledgement

Chao Yin is supported by China Scholarship Council (CSC). Zunchen Huang, Chenglu Jin and Marten van Dijk are (partly) supported by project CiCS of the research programme Gravitation, which is (partly) financed by the Dutch Research Council (NWO) under the grant 024.006.037. Fabio Massacci is supported by the Dutch Secutorplan.

References

[1] Mohamed El Massad, Siddharth Garg, and Mahesh V Tripunitara. 2015. Integrated circuit (IC) decamouflaging: Reverse engineering camouflaged ICs within minutes.. In *NDSS*. 1–14.

[2] Daniel Günther, Ágnes Kiss, Lukas Scheidel, and Thomas Schneider. 2019. Poster: Framework for semi-private function evaluation with application to secure insurance rate calculation. In *Proceedings of the 2019 ACM SIGSAC Conference on Computer and Communications Security*. 2541–2543.

[3] Daniel Günther, Joachim Schmidt, Thomas Schneider, and Hossein Yalame. 2024. FLUENT: A Tool for Efficient Mixed-Protocol Semi-Private Function Evaluation. *Cryptology ePrint Archive* (2024).

[4] Chenglu Jin, Chao Yin, Marten van Dijk, Sisi Duan, Fabio Massacci, Michael K Reiter, and Haibin Zhang. 2024. PG: Byzantine Fault-Tolerant and Privacy-Preserving Sensor Fusion With Guaranteed Output Delivery. In *Proceedings of the 2024 on ACM SIGSAC Conference on Computer and Communications Security*. 3272–3286.

[5] Jonathan Katz and Lior Malka. 2011. Constant-round private function evaluation with linear complexity. In *International Conference on the Theory and Application of Cryptology and Information Security*. Springer, 556–571.

[6] Carmen Kempka, Ryo Kikuchi, and Koutarou Suzuki. 2016. How to circumvent the two-ciphertext lower bound for linear garbling schemes. In *Advances in Cryptology–ASIACRYPT 2016: 22nd International Conference on the Theory and Application of Cryptology and Information Security, Hanoi, Vietnam, December 4–8, 2016, Proceedings, Part II 22*. Springer, 967–997.

[7] Vladimir Kolesnikov. 2018. Free IF: How to omit inactive branches and implement S-universal garbled circuit (almost) for free. In *International Conference on the Theory and Application of Cryptology and Information Security*. Springer, 34–58.

[8] Vladimir Kolesnikov and Thomas Schneider. 2008. A practical universal circuit construction and secure evaluation of private functions. In *Financial Cryptography and Data Security: 12th International Conference, FC 2008, Cozumel, Mexico, January 28–31, 2008. Revised Selected Papers 12*. Springer, 83–97.

[9] Ruixiao Li and Hayato Yamana. 2024. Non-interactive Private Multivariate Function Evaluation using Homomorphic Table Lookup. *IACR Communications in Cryptology* 1, 3 (2024).

[10] Ruixiao Li and Hayato Yamana. 2024. Privacy Preserving Function Evaluation Using Lookup Tables with Word-Wise FHE. *IEICE Transactions on Fundamentals of Electronics, Communications and Computer Sciences* 107, 8 (2024), 1163–1177.

[11] Ke Lin. 2023. Skipping Scheme for Gate-hiding Garbled Circuits. *arXiv preprint arXiv:2312.02514* (2023).

[12] Fabio Massacci and Laura Marraro. 2000. Logical cryptanalysis as a SAT problem. *Journal of Automated Reasoning* 24 (2000), 165–203.

[13] Payman Mohassel and Saeed Sadeghian. 2013. How to hide circuits in MPC an efficient framework for private function evaluation. In *Annual International Conference on the Theory and Applications of Cryptographic Techniques*. Springer, 557–574.

[14] Annika Paus, Ahmad-Reza Sadeghi, and Thomas Schneider. 2009. Practical secure evaluation of semi-private functions. In *Applied Cryptography and Network Security: 7th International Conference, ACNS 2009, Paris-Rocquencourt, France, June 2–5, 2009. Proceedings 7*. Springer, 89–106.

[15] Jeyavijayan Rajendran, Michael Sam, Ozgur Sinanoglu, and Ramesh Karri. 2013. Security analysis of integrated circuit camouflaging. In *Proceedings of the 2013 ACM SIGSAC conference on Computer & communications security*. 709–720.

[16] Mike Rosulek. 2017. Improvements for gate-hiding garbled circuits. In *Progress in Cryptology–INDOCRYPT 2017: 18th International Conference on Cryptology in India, Chennai, India, December 10–13, 2017, Proceedings 18*. Springer, 325–345.

[17] Mike Rosulek and Lawrence Roy. 2021. Three halves make a whole? Beating the half-gates lower bound for garbled circuits. In *Annual International Cryptology Conference*. Springer, 94–124.

[18] Hao Shen et al. 2025. Bootstrapping in approximate fully homomorphic encryption: a research survey. *Cybersecurity* (2025). doi:10.1186/s42400-025-00384-3

[19] Yuanqi Shen, Amin Rezaei, and Hai Zhou. 2018. SAT-based bit-flipping attack on logic encryptions. In *2018 Design, Automation & Test in Europe Conference & Exhibition (DATE)*. IEEE, 629–632.

[20] Pramod Subramanyan, Sayak Ray, and Sharad Malik. 2015. Evaluating the security of logic encryption algorithms. In *2015 IEEE International Symposium on Hardware Oriented Security and Trust (HOST)*. IEEE, 137–143.

[21] Yongge Wang and Qutaibah M Malluhi. 2024. Reducing garbled circuit size while preserving circuit gate privacy. In *International Conference on Cryptology in Africa*. Springer, 149–173.

[22] Yang Xie and Ankur Srivastava. 2016. Mitigating SAT attack on logic locking. In *Cryptographic Hardware and Embedded Systems–CHES 2016: 18th International Conference, Santa Barbara, CA, USA, August 17–19, 2016, Proceedings 18*. Springer, 127–146.

[23] Xiaolin Xu, Bicky Shakya, Mark M Tehranipoor, and Domenic Forte. 2017. Novel bypass attack and BDD-based tradeoff analysis against all known logic locking attacks. In *Cryptographic Hardware and Embedded Systems–CHES 2017: 19th International Conference, Taipei, Taiwan, September 25–28, 2017, Proceedings*. Springer, 189–210.

[24] Muhammad Yasin, Bodhisatwa Mazumdar, Jeyavijayan JV Rajendran, and Ozgur Sinanoglu. 2016. SARLock: SAT attack resistant logic locking. In *2016 IEEE International Symposium on Hardware Oriented Security and Trust (HOST)*. IEEE, 236–241.

[25] Cunxi Yu, Xiangyu Zhang, Duo Liu, Maciej Ciesielski, and Daniel Holcomb. 2017. Incremental SAT-based reverse engineering of camouflaged logic circuits. *IEEE Transactions on Computer-Aided Design of Integrated Circuits and Systems* 36, 10 (2017), 1647–1659.

[26] Mingfei Yu and Giovanni De Micheli. 2026. Faster Homomorphic Operations and Beyond: Expediting Homomorphic Computation via Boolean Circuit Optimization: M. Yu, G. De Micheli. *Journal of Cryptology* 39, 1 (2026), 6.

[27] Shuoyao Zhao, Yu Yu, Hanlin Liu, Jiang Zhang, Wenling Liu, and Zhenkai Hu. 2024. Improving the Efficiency of Private Function Evaluation Via Optimized Universal Circuits. *IEEE Transactions on Dependable and Secure Computing* (2024).

[28] Hai Zhou, Rui Feng Jiang, and Shuyu Kong. 2017. CycSAT: SAT-based attack on cyclic logic encryptions. In *2017 IEEE/ACM International Conference on Computer-Aided Design (ICCAD)*. IEEE, 49–56.

[29] Hayo Zhu, Takuya Suzuki, and Hayato Yamana. 2025. Private Function Evaluation using CKKS-based Homomorphic Encrypted LookUp Tables. In *2025 22nd Annual International Conference on Privacy, Security, and Trust (PST)*. IEEE, 1–10.

A Proofs

We first define a set of special type set operators which will facilitate the following proofs of Theorem 4.1 and 4.5, and then we prove the correctness of these two theorems.

A.1 Type Set Operators

Operators on type sets: For a type set \mathcal{T} we define the set of gates that negates the output wire of a gate in \mathcal{T} as

$$\overline{\mathcal{T}} = \{ \text{NOT } g : g \in \mathcal{T} \}.$$

Each gate in \mathcal{T} has two input wires, a left input wire and a right input wire. The following sets extend \mathcal{T} by possibly negating the left and/or right input wire:

$$\begin{aligned} \underline{\mathcal{T}} &= \mathcal{T} \cup \{ g(\text{NOT } A, B) : g \in \mathcal{T} \}, \\ \underline{\mathcal{T}}_o &= \mathcal{T} \cup \{ g(A, \text{NOT } B) : g \in \mathcal{T} \}, \\ \underline{\mathcal{T}}_o &= \mathcal{T} \cup \{ g(\text{NOT } A, \text{NOT } B) : g \in \mathcal{T} \} \\ &\quad \cup \{ g(A, \text{NOT } B) : g \in \mathcal{T} \} \\ &\quad \cup \{ g(\text{NOT } A, \text{NOT } B) : g \in \mathcal{T} \}. \end{aligned}$$

When we write $\mathcal{T} = \mathcal{T}'$ for two type sets \mathcal{T} and \mathcal{T}' , then we mean that the two type sets provide gates with *equal functionality*. For example, let \mathcal{L} be the full set of 16 types. Notice that

$$\overline{\mathcal{L}} = \mathcal{L} = \underline{\mathcal{L}} = \underline{\mathcal{L}}_o = \underline{\mathcal{L}}_o$$

where equations relate to functionality.

The following sets extend \mathcal{T} by possibly replacing the left and/or right input wire by TRUE:

$$\begin{aligned} {}_T \underline{\mathcal{T}} &= \mathcal{T} \cup \{g(\text{TRUE}, B) : g \in \mathcal{T}\}, \\ \underline{\mathcal{T}}_T &= \mathcal{T} \cup \{g(A, \text{TRUE}) : g \in \mathcal{T}\}, \\ {}_T \underline{\mathcal{T}}_T &= \mathcal{T} \cup \{g(\text{TRUE}, B) : g \in \mathcal{T}\} \\ &\cup \{g(A, \text{TRUE}) : g \in \mathcal{T}\} \\ &\cup \{g(\text{TRUE}, \text{TRUE}) : g \in \mathcal{T}\}. \end{aligned}$$

A.2 Proof of Theorem 4.1

R-Wave Simplification: Let

$$\mathcal{R} = \{\text{XOR, OR, A} \Rightarrow \text{B, B} \Rightarrow \text{A, NAND, TRUE, NOT A, NOT B}\} \text{ and}$$

$$\overline{\mathcal{R}} = \{\text{XNOR, NOR, A AND (NOT B), (NOT A) AND B, AND, FALSE, A, B}\}.$$

Initially, each circuit gate g is in \mathcal{L} and we have not assigned any new type set to any gate of the circuit. Let R be the set of gates that have been assigned type set \mathcal{R} – initially, $R = \emptyset$. We will one by one consider all the gates of the circuit, except those in the primary output layer, and add these to R . This procedure will have as invariant that if a gate $g \in R$, then if an input wire of g connects to a gate g' , then $g' \in R$ (this is for both input wires of g).

As long as there is a gate $g \notin R$ with each of its input wires either from R or from an actual input to the circuit, and g is not in the primary output layer of the circuit, we do the following: Since $g \notin R$, g still has type set \mathcal{L} assigned to it. Since $\mathcal{L} = \mathcal{R} \cup \overline{\mathcal{R}}$, either $g \in \mathcal{R}$ or $g \in \overline{\mathcal{R}}$. In the latter case we restrict $g \in \mathcal{R}$ and push the negation of the output wire to all the gates that it connects to as an input wire. This is possible since g is not in the output layer of the circuit. We assign type set \mathcal{R} to gate g and we add g to set R . Notice that g is chosen in such a way that the invariant again holds.

We need to check the effect of pushing possible negations through the output wire of g . Each of the gates that the output wire connects to (it may have fanout > 1) is not in R (by our invariant) and such gates have still type set \mathcal{L} assigned to them. Such a gate can therefore absorb negations that come over its input wires because $\mathcal{L} = \mathcal{L}$. This shows that after re-assigning g to type set \mathcal{R} , we still obtain a functionally equivalent circuit.

Assume that there only exist gates $g \notin R$ outside the primary output layer that have at least one of its input wires not from a gate in R and not from an actual input to the circuit. Then that input wire connects as an output wire to another gate $g' \notin R$ which is outside the primary output layer. According to our assumption, this gate g' connects through one of its input wires to another gate $g'' \notin R$ outside the primary output layer, and so on. Since the circuit has no loops and is finite, this leads to a contradiction. We conclude that our assumption is wrong. Therefore, as long as there exists a gate $g \notin R$ outside the primary output layer, then there also exists a gate $g \notin R$ outside the primary output layer with each of its input wires either from R or from an actual input to the circuit. This means that when our R-Wave simplification ends, there are no more gates $g \notin R$ outside the primary output layer

and we have arrived at an equivalent circuit where each gate that is not part of the primary output layer is in \mathcal{R} .

A.3 Proof of Theorem 4.5

S-Class Simplification: An S-Class gate is a non-input-layer gate whose two input wires each originate from a source with fanout = 1. To analyze their interconnections, we form a directed graph whose nodes are exactly the S-Class gates. We draw an edge from gate g to gate h if and only if the output wire of a fanout = 1 gate g feeds into h . Because the original circuit's graph is acyclic, this induced subgraph on S-Class gates is also acyclic. Hence, this graph naturally decomposes into a forest of directed trees, each tree forming an S-Class subtree of connected S-Class gates (which may be a lone node/gate, a linear chain, or a branching binary tree) within the larger circuit structure. In this S-Class graph, each node/gate has at most one outgoing edge and up to two incoming edges from other S-Class gates. Nodes without any outgoing edge serve as the roots of their belonging subtree. In this section, we analyze how the type sets for gates in an S-Class subtree can be further simplified.

Let us consider one of the S-Class subtree. We first consider its root. The root gate starts with type set \mathcal{L} .

$$\begin{aligned} \mathcal{L} &= \underline{\{\text{XOR}\}} \cup \underline{\{\text{AND}\}} \cup \underline{\{\text{NAND}\}} \\ &\cup \{\text{TRUE, NOT A, NOT B}\} \cup \{\text{FALSE, A, B}\} \\ &= \underline{\{\text{XOR}\}} \cup \underline{\{\text{AND}\}} \cup \underline{\{\text{NAND}\}} \\ &\cup {}_T \underline{\{\text{AND}\}}_T \cup {}_T \underline{\{\text{NAND}\}}_T \\ &= \underline{\{\text{XOR, AND, NAND}\}} \cup {}_T \underline{\{\text{AND, NAND}\}}_T. \end{aligned} \quad (1)$$

From decomposition (1), we infer that we may restrict the root gate to type set

$$\mathcal{S} = \{\text{XOR, NAND, AND}\}$$

if we appropriately modify the gates g_a and g_b which provide output wires with fanout=1 that serves as input wires A and B, respectively, to the root gate. These modifications for g_a and g_b can be no change to the type, a negation of the type, or replacing the type with TRUE.

Now we consider the non-root gates of the subtree. Our aim is to restrict their types preferably to type set \mathcal{S} . Initially, we already accomplished this for the root gate.

Let Q be a subtree of our subtree including the root gate. As an induction hypothesis we have that all the gates in Q are restricted to \mathcal{S} . We start with Q consisting only of the root gate – our induction hypothesis holds. We extend Q with a new gate g from our subtree. We remind the reader that g is in the type set \mathcal{L} initially. After applying the appropriate changes required by its preceding gate, which is in \mathcal{S} , g will still be within the type set \mathcal{L} . Thus, we can reapply the decomposition (1) of type set \mathcal{L} , and reassign the type of g to type set \mathcal{S} if we appropriately modify its input gates. By induction, we have reassigned the types of all the gates in the subtree to \mathcal{S} . Also, the gates that provide input wires with fanout=1 to the subtree remain in \mathcal{L} of 16 types to these gates after the required changes from the subtree.

Z-Class simplification: Z-Class gates are defined as those gates that are not part of the first input layer of the circuit and have exactly one input wire with fanout=1 (the other input wire has fanout > 1). We create a directed acyclic graph where the nodes represent all Z-Class gates and where the directed edges from one node/gate to another node/gate are output wires with fanout=1. By the definition of Z-Class gates, each Z-Class gate can have at most 1 incoming wire from another Z-Class gate and can have at most 1 outgoing wire to another Z-Class gate. The circuit topology has no loops, and therefore our directed graph is a union of disconnected line graphs (and is acyclic). Each line graph has its edges pointing from a bottom node to a root node; their directions are all lined up. Within the circuit topology, the line graph zigzags; sometimes an edge represents an output wire that is equal to a left input wire, and other times an edge represents an output wire that is equal to a right input wire. Notice that zigzag line graphs and subtrees do not intersect because Z-Class gates are different from S-Class gates.

Because Z-Class gates never overlap with S-Class gates, and because after S-Class simplification every non-subtree gate still retains the full type set \mathcal{L} , it follows that the root of any Z-Class zigzag chain must itself belong to \mathcal{L} .

$$\begin{aligned}
 \mathcal{L} &= \underline{\text{XOR}} \cup \underline{\text{AND}} \cup \underline{\text{NAND}} \cup \underline{\text{NOR}} \cup \\
 &\quad \underline{\text{OR}} \cup \{\text{TRUE, NOT A, NOT B}\} \cup \{\text{FALSE, A, B}\} \\
 &= \underline{\text{XOR}} \cup \underline{\text{AND}} \cup \underline{\text{NAND}} \cup \underline{\text{NOR}} \cup \\
 &\quad \underline{\text{OR}} \cup \{\text{TRUE, FALSE}\} \cup \underline{\text{B}} \cup \underline{\{\text{AND}\}}_T \cup \underline{\{\text{NAND}\}}_T \\
 &= \underline{\{\text{XOR, AND, NAND, NOR, OR, B}\}} \cup \{\text{TRUE, FALSE}\} \\
 &\quad \cup \underline{\{\text{AND, NAND}\}}_T \\
 &= \underline{\{\text{XOR, AND, NAND, NOR, OR, B}\}} \\
 &\quad \cup \underline{\{\text{OR, NOR, AND, NAND}\}}_T. \tag{2}
 \end{aligned}$$

and similarly,

$$\begin{aligned}
 \mathcal{L} &= \underline{\{\text{XOR, AND, NAND, NOR, OR, A}\}} \\
 &\quad \cup \underline{\{\text{OR, NOR, AND, NAND}\}}. \tag{3}
 \end{aligned}$$

From the decompositions (2) and (3) of \mathcal{L} we replace the type set of g_b (or g_a if the root gate has a left input wire with fanout=1) with

$$\begin{aligned}
 \mathcal{Z}_{\text{right}} &= \{\text{XOR, AND, NAND, NOR, OR, B}\} \text{ or} \\
 \mathcal{Z}_{\text{left}} &= \{\text{XOR, AND, NAND, NOR, OR, A}\}
 \end{aligned}$$

depending on whether g_b has a right input wire with fanout=1 or a left input wire with fanout=1. Both these type sets have size 6.

We may now continue reasoning in the way we have done for the S-Class subtree simplification and assign all the nodes in the Z-class zigzag line to the type set $\mathcal{Z}_{\text{right}}$ or $\mathcal{Z}_{\text{left}}$, and the gates that provide inputs to the last node of the Z-class zigzag line will stay in \mathcal{L} after having adapted one of the required changes: no change of its type, a negation of its type, or a TRUE assignment.

When assigning these type sets to the last node, then the reasoning of the S-Class subtree simplification assumes that it connects

Algorithm 3 Baseline SAT-based Function Recovery Algorithm (Details)

Require: Circuit Topology τ , Oracle_f(\cdot)
Ensure: Equivalent gate-type assignment \mathcal{T}

- 1: $DI \leftarrow \emptyset, F_{\text{Block}} \leftarrow \text{True}$
- 2: **while** True **do**
- 3: $F_{\text{two}} \leftarrow \text{EncodeTwoCircuit}(\tau, T_1, T_2, DI) \wedge$
 $\wedge \text{DiffConstr}(\tau, T_1, T_2, X) \wedge F_{\text{Block}}$
- 4: **if** F_{two} is SAT **then**
- 5: Solve F_{two} to obtain $X \leftarrow \mathbf{x}, T_1 \leftarrow \mathcal{T}_1, T_2 \leftarrow \mathcal{T}_2$
- 6: $\mathbf{z} \leftarrow \text{Oracle}_f(\mathbf{x})$, update $DI \leftarrow DI \cup \{(\mathbf{x}, \mathbf{z})\}$
- 7: $C_1 \leftarrow (\tau, \mathcal{T}_1), C_2 \leftarrow (\tau, \mathcal{T}_2)$
- 8: **if** $\text{Eval}(C_1)(\mathbf{x}) \neq \mathbf{z}$ **then**
- 9: $F_{\text{Block}} \leftarrow F_{\text{Block}} \wedge \bigwedge_{i \in 1,2} \text{BlockCirc}(T_i, \mathcal{T}_1)$
- 10: **end if**
- 11: **if** $\text{Eval}(C_2)(\mathbf{x}) \neq \mathbf{z}$ **then**
- 12: $F_{\text{Block}} \leftarrow F_{\text{Block}} \wedge \bigwedge_{i \in 1,2} \text{BlockCirc}(T_i, \mathcal{T}_2)$
- 13: **end if**
- 14: **else** break
- 15: **end if**
- 16: **end while**
- 17: $F_{\text{one}} \leftarrow \text{EncodeCircuit}(\tau, T, DI)$
- 18: Solve F_{one} to obtain $T \leftarrow \mathcal{T}$
- 19: **return** \mathcal{T}

through its input wire with fanout=1 to a gate with type set \mathcal{L} , which contains the type TRUE so that it can absorb the needed TRUE assignments to that input wire. However, the above Z-Class simplification can connect through its input wire with fanout=1 of the last node to either a gate with type set \mathcal{L} or to a subtree root which has type set \mathcal{S} and does not contain TRUE. This is not a cause for concern because the subtree as a whole, together with the gates that provide input over the fanout=1 input wires to the subtree does allow the TRUE gate functionality by setting all those gates that provide input to the subtree to type TRUE. This is possible if those gates all have type set \mathcal{L} . However, such a gate may be a root of a zigzag line graph. In the latter case we cannot directly assign this to the TRUE type. However, we may follow this zigzag line graph again to its last node. And again, we may enter a subtree and so on. At some moment, we reach the primary input layer of the circuit with its gates (by definition not S-Class or Z-Class gates) all assigned to type set \mathcal{L} which contains TRUE.

B Detailed Pseudocodes

Here, we provide detailed pseudocodes for the baseline attack (Algorithm 3) and our optimized attack (Algorithm 4).

C Theoretical Analysis of Search-Space Reduction

We have described both the baseline and improved recovery algorithms. We now present a theoretical analysis that explains why the proposed simplification rules and the resulting reduction of gate-type ambiguity lead to significant improvements in solver performance.

Algorithm 4 Enhanced SAT-based Function Recovery Algorithm (with Simplification Theorems)

```

Require: Circuit topology  $\tau$ , Oracle  $\text{Oracle}_f(\cdot)$ 
Ensure: Equivalent gate-type assignment  $\mathcal{T}$ 
1:  $DI \leftarrow \emptyset$ ,  $F_{GBlock} \leftarrow \text{True}$ ,  $\text{LabelList} \leftarrow \text{ClassifyGates}(\tau)$ 
2: while true do ▷ repeat until  $DI$  is complete
3:    $F_{\text{one}} \leftarrow \text{EncodeCircuit}(\tau, T, DI, \text{LabelList}) \wedge F_{GBlock}$ 
4:   if  $F_{\text{one}}$  is UNSAT then break
5:   end if
6:   Solve  $F_{\text{one}}$  for  $\mathcal{T}_1$  ▷ Find 1st gate-type assignment
7:    $F_{\text{one}} \leftarrow F_{\text{one}} \wedge \text{BlockCirc}(T, \mathcal{T}_1)$ 
8:    $\text{countInnerIter} \leftarrow 0$ 
9:   while  $F_{\text{one}}$  is SAT do
10:    Solve  $F_{\text{one}}$  for  $\mathcal{T}_2$  ▷ Find 2nd gate-type assignment
11:     $F_{\text{dis}} \leftarrow \text{DiffConstr}(\tau, \mathcal{T}_1, \mathcal{T}_2, X)$ 
12:    if  $F_{\text{dis}}$  is SAT then
13:      Solve  $F_{\text{dis}}$  for a new discriminating input vector  $\mathbf{x}$ 
14:       $\mathbf{z} \leftarrow \text{Oracle}_f(\mathbf{x})$ , update  $DI \leftarrow DI \cup \{(\mathbf{x}, \mathbf{z})\}$ 
15:       $C_1 \leftarrow (\tau, \mathcal{T}_1), C_2 \leftarrow (\tau, \mathcal{T}_2)$ 
16:      for  $j = 1, 2$  do
17:        if  $\text{Eval}(C_j)(\mathbf{x}) \neq \mathbf{z}$  then
18:           $F_{GBlock} \leftarrow F_{GBlock} \wedge \text{BlockCirc}(T, \mathcal{T}_j)$ 
19:        end if
20:      end for
21:      break inner while
22:    else ▷ Block  $\mathcal{T}_2$  within the current inner loop
23:       $\text{countInnerIter} \leftarrow \text{countInnerIter} + 1$ 
24:      if  $\text{countInnerIter} \geq N_{\text{max}}$  then
25:         $F_{\text{two}} \leftarrow \text{EncodeTwoCircuit}(\tau, \mathcal{T}_1, \mathcal{T}_2, DI) \wedge$ 
26:         $\wedge \text{DiffConstr}(\tau, \mathcal{T}_1, \mathcal{T}_2, X) \wedge F_{GBlock}$ 
27:        if  $F_{\text{two}}$  is SAT then
28:          Solve  $F_{\text{two}}$  to obtain  $X \leftarrow \mathbf{x}, T_2 \leftarrow \mathcal{T}_2$ 
29:           $\mathbf{z} \leftarrow \text{Oracle}_f(\mathbf{x})$ , update  $DI \leftarrow DI \cup \{(\mathbf{x}, \mathbf{z})\}$ 
30:          break inner while
31:        else
32:          break outer while
33:        end if
34:       $F_{\text{one}} \leftarrow F_{\text{one}} \wedge \text{BlockCirc}(T, \mathcal{T}_2)$ 
35:      continue inner while
36:    end if
37:  end while
38:  if  $F_{\text{one}}$  is UNSAT then break outer while
39:  end if
40: end while
41:  $F_{\text{final}} \leftarrow \text{EncodeCircuit}(\tau, T, DI, \text{LabelList}) \wedge F_{GBlock}$ 
42: Solve  $F_{\text{final}}$  for  $\mathcal{T}$ 
43: return  $\mathcal{T}$ 

```

C.1 Effect on SAT Structural Complexity

The SAT encoding introduced in Section 5 represents the gate type at each gate $g \in \mathcal{N}$ using one-hot type-selection variables. For each admissible type $t \in D(g)$, a Boolean selector variable $\text{Sel}_{g,t}$ is introduced, together with an exactly-one constraint over the set $\{\text{Sel}_{g,t} \mid t \in D(g)\}$. In the baseline formulation we have $D(g) = \mathcal{L}$

for all g , while the R+S+Z simplification of Section 4 reduces $D(g)$ to smaller subsets such as \mathcal{S} , $\mathcal{Z}_{\text{left}}$, $\mathcal{Z}_{\text{right}}$, or \mathcal{R} .

Let

$$b_{\text{full}} = \sum_{g \in \mathcal{N}} |\mathcal{L}| \quad \text{and} \quad b_{\text{shrunken}} = \sum_{g \in \mathcal{N}} |D(g)|$$

denote the total numbers of type-selection variables in the full and simplified domains. The simplification rules therefore reduce the number of type variables from b_{full} to b_{shrunken} . This reduction directly shrinks the width and number of the one-hot clauses: for each gate g , the at-least-one clause has width $|D(g)|$, and the at-most-one constraints contain $O(|D(g)|^2)$ binary clauses. After simplification, both the size and the density of these constraint blocks become smaller.

The selector variables $\text{Sel}_{g,t}$ also participate in the functional constraints that link the type choice of g to its input and output signal variables $v_g^{(i)}$ across all samples. These constraints introduce edges between type-selection variables and signal variables in the primal graph of the CNF. When $D(g)$ is reduced, fewer selector variables connect to each functional-constraint block, which lowers the interaction degree of g in the primal graph and reduces the number of potential resolution steps involving type and signal literals. Consequently, the CNF instances produced after simplification have strictly fewer type-related variables, fewer type–signal interaction clauses, and smaller one-hot clusters.